Thermodynamic assessment of downhole heat exchangers for geothermal power generation

Nurdan Yildirim [a, *], Slamet Parmanto [b], Gulden Gokcen Akkurt [c]

[a] Department of Energy Systems Engineering, Yasar University, Universite Caddesi, No: 37-39, Bornova 35100 Izmir, Turkey
[b] Department of Mechanical Engineering, Izmir Institute of Technology, Urla, Izmir, Turkey
[c] Department of Energy Systems Engineering, Izmir Institute of Technology, Urla, Izmir, Turkey

ABSTRACT

Downhole heat exchanger is a device to extract heat from geothermal fluid. While it is widely used for heating purposes, its use for power generation has not been reported. The aim of this study is to examine the feasibility of power generation from a 2500 m deep existing geothermal well with high temperature gradient and insufficient flowrate by using a downhole heat exchanger. For this purpose, a thermodynamic and an economic evaluation model are developed by the use of Engineering Equation Solver software. Additionally, the parametric studies have been carried out to identify the effects of insulation, geothermal well conditions, geometry of downhole heat exchanger, mass flowrate and type of working fluids on the performance of downhole heat exchanger system. Consequently, work output of the best alternative is computed as 2511 kW$_e$ with 64 kg/s mass flowrate of R-134a for 2500 m-deep downhole heat exchanger having inner pipe diameter of 0.127 m. Electricity generation cost and simple payback time are calculated as 46 $/MWh and 2.25 years, respectively. The obtained results showed that the downhole heat exchanger system can be a feasible alternative for wells with very low geothermal flowrate to generate power.

© 2019 Elsevier Ltd. All rights reserved.

1. Introduction

Conventional and binary geothermal power plants (GPPs) require sufficient geothermal flowrate along with the temperature for a feasible operation. If geothermal fields have high temperatures but low or no flowrate, they are called as Hot Dry Rock (HDR) systems. HDR systems exist in many places around the World and it is estimated that they contain 800 times higher energy than all hydrothermal resources at economical depths [1]. To be able to harness energy stored in those systems, two deep wells are drilled, then water is injected down through injection wells where its pressure increases in naturally fractured rocks, passes through the hot rock, then returns back to the surface by production well with an increase in temperature. After extracting its useful energy, water is re-injected back to the injection well, hence completing the cycle (Fig. 1).

This type of geothermal energy extraction is known as Enhanced Geothermal Systems (EGS). Besides EGSs, Downhole Heat

Exchangers (DHEs) can be applied to HDR systems. A DHE is designed to move the heat extraction process into geothermal well. The working fluid is injected down to DHE, which suspends in the geothermal well, heated by geothermal fluid and returned back to the surface (Fig. 2). Currently, this technology is applied to produce heat for direct use applications such as space heating, bathing, industrial process heating and snow melting but not for power generation. Installed capacity of DHEs used for direct use applications were 70,328 MW$_t$ (163,287 GWh/year) in 2015 which grew 1.62 times compared to installed capacity in 2010 [3].

Besides direct use applications, DHEs can be a good alternative to generate power from geothermal resources with high temperature but low flowrate. Alimonti et al. (2018) reviewed DHEs technically and concluded that using DHE systems, it could be possible to produce thermal and electric power in a range of 0.15—2.5 MW$_t$ and 0.25—364 kW$_e$, respectively [4].

DHEs have several advantages in extracting heat from the reservoir such as eliminating the problems of geothermal fluid discharge (corrosion and scaling problems) and drilling re-injection wells. Furthermore, DHEs have a simpler design than binary GPPs which reduce total investment cost. However, DHEs suffer from

---

* Corresponding author.
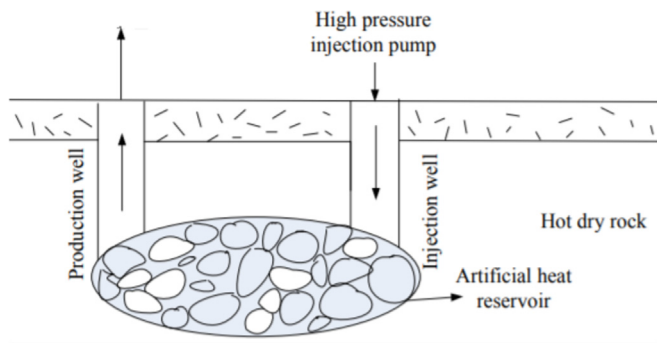*E-mail address:* nurdan.yildirim@yasar.edu.tr (N. Yildirim).

Fig. 1. Hot dry rock system [2].

limited heat output compared to conventional downhole pump systems, since flowrate is limited by the geometry of DHE. Therefore, to be able to obtain maximum heat output from a DHE, optimum pipe diameters and best performing working fluids should be determined.

Among the types of DHEs, U-type design is the most common type of DHE applications (Fig. 2, a). It consists of a pipe with U shape, which is suspended in the geothermal well. Heat from the well is extracted and conveyed to the surface by a working fluid that is first injected into the U shape pipe. Promoter pipes are designed to increase heat output from a DHE system. Natural convection circulates the geothermal fluid through the perforations of the pipe [5,6]. Spitler et al. (2016) studied groundwater-filled, 80 m deep well with a single U-tube, experimentally. An ethanol-water mixture with an ethanol concentration of 26.4% by weight was used as working fluid in the U-tube. Heat injection rates between −45 and 75 W/m were obtained by performing heat injection and heat extraction tests [7]. A feasibility study has been conducted about heat extraction from an abandoned oil well by Gharibi et al. (2018). The authors simulated a U-tube DHE under both steady- and unsteady-state conditions using actual geothermal field data. Outlet temperature of one of their scenarios

reached 114.9 °C at 0.5 m/s of water inlet velocity and 30 °C of inlet temperature. They concluded that 48.8 kW$_t$ gross heat power could be produced by this single well with 0.01 m pipe diameter and a thermal gradient of 3.14 °C/100 m [8].

A multi-tube DHE consists of a shell with a bundle of tubes inside (Fig. 2, b). While working fluid runs through the tubes, geothermal fluid flows in the shell. This type is capable of extracting more heat than U-type but causes a relatively high-pressure loss [9].

Coaxial DHE consist of an inner steel pipe that is covered by an annulus pipe as casing (Fig. 2, c). Based on the pipe which working fluid is injected down, the flow called forward and reverse flow. In forward flow, working fluid is injected down through the inner pipe and returns back to the surface from the annulus pipe after being heated by a hot rock or geothermal fluid. In reverse flow, the working fluid flows down through the annulus and goes up through the inner pipe. One of the advantages of coaxial DHEs over U-type is the operation with higher flowrates.

Acuña (2010) compared the performance of a U-type and a coaxial DHE. The results indicated that the coaxial DHE decreased pressure drop by 65% at a variety of flowrates compared with U-type [11]. Additionally, Zanchini et al. (2010) studied the effect of reverse and forward flow configuration of a coaxial DHE. The study concluded that reverse flow has greater heat transfer rate comparing with forward flow [12].

The studies showed that an increase in energy extraction rate can also be achieved by an increase in geothermal resource temperature, well diameter and mass flowrate through DHE [5,6]. Song et al. (2018) studied the closed loop geothermal system (CLGS) with working fluid of CO_2 and investigated effects of flowrate, inlet temperature, length of the horizontal section, and wellbore size, on the heat extraction performance of CLGS. The authors suggested that higher thermal power and outlet temperature could be possible with a geothermal fluid inlet temperature range of 30−40 °C [13]. Jiang et al. (2016) studied 4000 m-length multiple horizontal wells technology to extract more energy from the 4000 m-deep of the Earth. They used CO_2 as working fluid and concluded
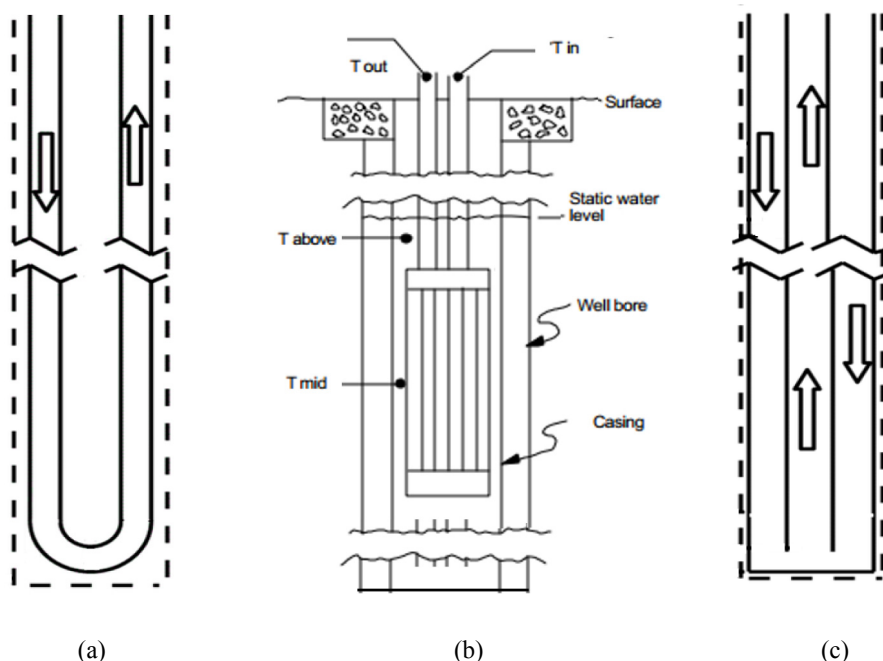

Fig. 2. Types of DHEs; (a) U-type [10], (b) multi-tube [6], (c) coaxial [10].

that thermodynamic properties of the horizontal well system were 38.9 °C and 10.9 MPa higher than the fractured reservoir system [14]. Falcone et al. (2018) conducted numerical simulations of a modified DHE which has addition of fillers to increase heat transfer. Encouraging results were obtained but further research was recommended [15].

Abandoned oil wells generally have fresh water at certain temperature with low mass flowrate but high temperature gradient and these wells may be used with the help of DHE applications to extract their power. Alkhasov et al. (2008) investigated the possibility of using abandoned oil wells at Yuzhno-Sukhokumsk-Dagestan with a depth of 800−900 m to meet the heat demand of a nearby municipality. A DHE system was installed to a 3000 m deep abandoned oil well and working fluid temperature was increased from 50 °C to 110 °C which was more than enough for heating purposes [16].

Nalla et al. (2005) studied the potential of DHEs for power generation by considering parametric-sensitivity studies of operational and design parameters of DHEs such as; geometry, working fluid properties, circulation flowrates and well properties including basal heat flux, and rock formation type. The study showed that working fluid residence time, heat transfer contact area and thermal properties of rock formation have significantly contributed to heat extraction rate [17].

Feng (2012) investigated the feasibility of power generation from low enthalpy geothermal resources by a long horizontal DHE. The study provided three main controls; increasing the length of DHE that enhances the heat exchange area by prolonging the residence time of working fluid, increasing mass flowrate of working fluid and increasing geothermal fluid flowrate that increases heat transfer rate of the system [18]. A coaxial DHE inside a horizontal borehole coupled with binary power plant was studied by Feng et al. (2015). The results of thermodynamic analysis showed that approximately 350 kW$_e$ power can be generated by this system [19].

Moreover, Akhmadullin and Tyagi (2014) evaluated the effect of working fluid type based on high thermal conductivity, high heat transfer and safety. The authors concluded that n-pentane with mass flowrate of 4.53 kg/s is the most suitable working fluid among other working fluids. They also summarized that working fluid selection depends on the individual project parameters such as application type, scheme configuration, temperature gradient and pressure variations. Although there is no exact way for the refrigerant selection, cycle optimization can help the right selection [20].

Pumping is required to circulate and to pressurize working fluid when it is injected to DHE. But, circulation pumps always consume energy so that influences net work output. In order to increase net work output, Morita et al. (2005) studied on minimizing circulation pump power. Diameter of the well and inner pipe is a critical factor on pressure drop. The study concluded that the gravity head which arises in DHE is possible to substitute pump function on circulating the working fluid [21].

The influence of working fluid on low to medium temperature Organic Rankine Cycle (ORC) were investigated widely [22−25]. Kilicarslan and Müller (2005) presented that water is a natural working fluid with high heat content potential. But water has several disadvantages such as high specific volume, high pressure ratio and high compressor outlet temperatures when compared to other working fluids (R717, R290, R134a, R12, R22, and R152a) [22]. Anh (2009) studied several criteria for selection of working fluid such as thermal efficiency, stability, compatibility with contacted materials in the cycle, safety, health and environmental effects. In the study; hydrocarbons, alkanes, aromates, siloxanes, and cycloalkanes were selected for their performance based on the above-mentioned criteria. Furthermore, the study showed that investigated alkanes, cyclopentane, toluene and o-xclene have the highest potential depending on the working fluid temperature range [23]. The effect of various refrigerants on the efficiency of geothermal power cycles were investigated by Masheiti et al. (2011) and Redko et al. (2016). Both studies concluded that the refrigerant R-245fa had a better performance [24,26].

The primary aim of this study is to develop a DHE model for power generation from high temperature but low mass flowrate geothermal resources. The objectives are to simulate the developed model thermodynamically based on DHE characteristics, well characteristics and working fluid characteristics by using an actual geothermal well at a 2500 m depth and a temperature gradient of 6 °C/100 m.
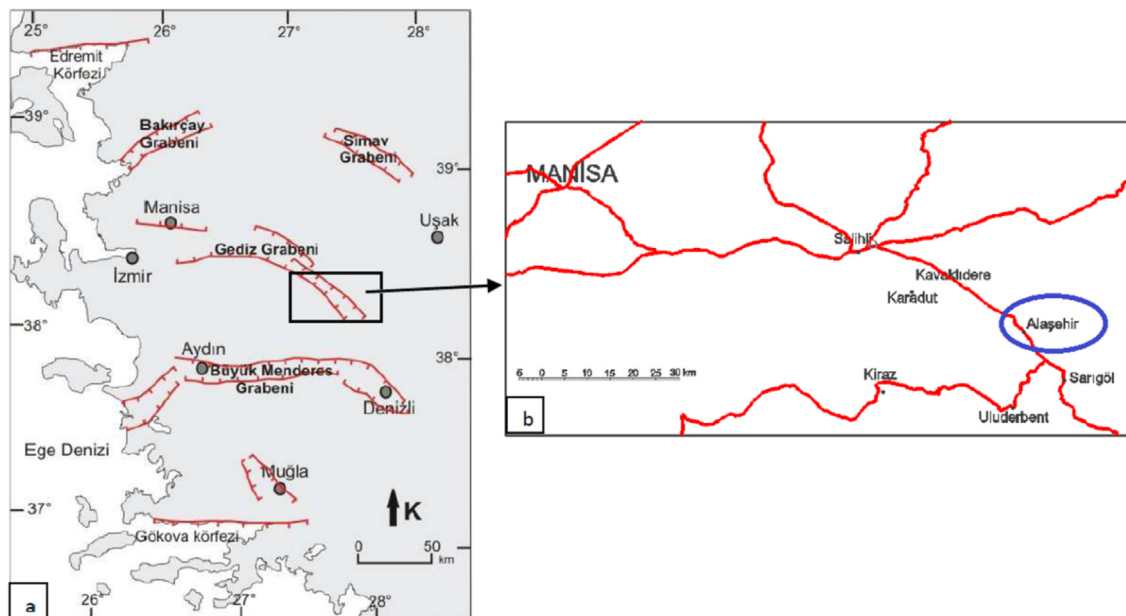

Fig. 3. a) Main tectonic elements of Western Anatolia-Turkey, b) Location of Alasehir Geothermal Field-Manisa, Turkey [28].
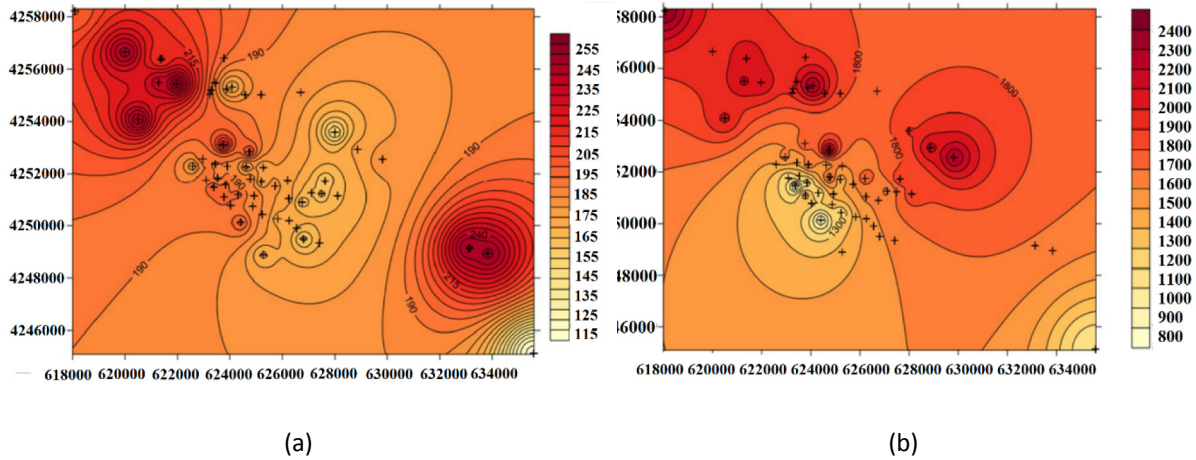
Fig. 4. Alasehir Geothermal Field. a) Reservoir temperatures (°C), b) Reservoir depths (m) [30].

2. Study site

Western Anatolia is one of the areas with highest geothermal potential of Turkey. Many geothermal resources occur along the Gediz Graben at locations of Turgutlu, Salihli and Alaşehir Geothermal Fields in Western Anatolia. The Alasehir Geothermal Field has become attractive for exploration and exploitation studies in the last 10 years following the discovery of the highest geothermal fluid temperature of 287 °C at 2750 m depth (Fig. 3) [27].

The field houses more than 100 geothermal wells serving 10 geothermal power plants with a total capacity of 206 MW$_e$ [29]. The temperatures in the field changes from 30 to 55 °C in hot springs and from 51 °C to 287 °C in geothermal wells. Fig. 4 gives reservoir temperature and depth data of Alasehir Geothermal Field. The figure indicates high heat flux of the field with a geothermal gradient as high as 10 °C/100 m. However, their discharges are between 2 and 80 l/s [30].

The geothermal well, used in this study is located in Alasehir Geothermal Field, has a geothermal gradient of 6 °C/100 m (Fig. 5).

3. System description

The GPP-DHE consists of two sections; a DHE (I) and power plant (II), as shown in Fig. 6. The DHE (I) is a heat exchanger that extracts heat from a geothermal heat source and the binary type power plant (II) converts the extracted heat into useful work (electricity).
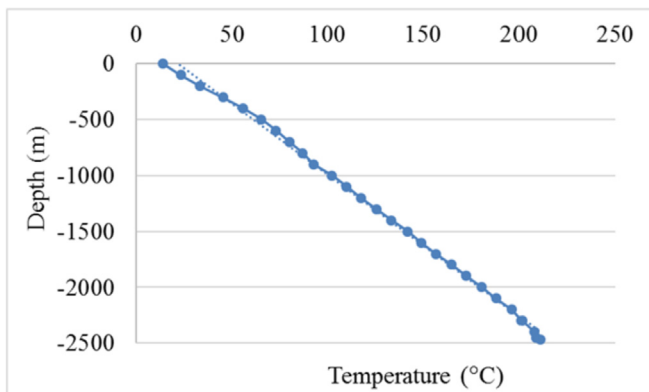
Schematic view of the DHE is shown in Fig. 7. Type of DHE is chosen as coaxial for its better performance and lower pressure drop comparing with other types and configurations [11].

The direction of the working fluid is the reverse direction where cold working fluid enters the annulus and exits through the inner pipe. The inner pipe is insulated by glass wool to avoid temperature decrease at the DHE exit caused by heat loss from the working fluid. A corrugated plastic pipe is added to protect the insulation from the working fluid.

The geothermal fluid in the well is not flowing but assumed as there is natural convection because of the changing temperature through the depth. Temperature gradient of the geothermal fluid in the existing well which is 6 °C/100 m, is used for analysis. The diameter of the existing geothermal well is 0.254 m. Depending on the well diameter, annulus diameter is fixed as 0.2032 m. Length of DHE, inner tube diameter and pipe materials are taken as variables to evaluate their effect on heat extraction rate.

4. Methodology

Thermodynamic and economic models are developed for GPP-DHE shown in Fig. 6. The code is written in Engineering Equation Solver (EES) [32] which has a high accuracy thermodynamic and
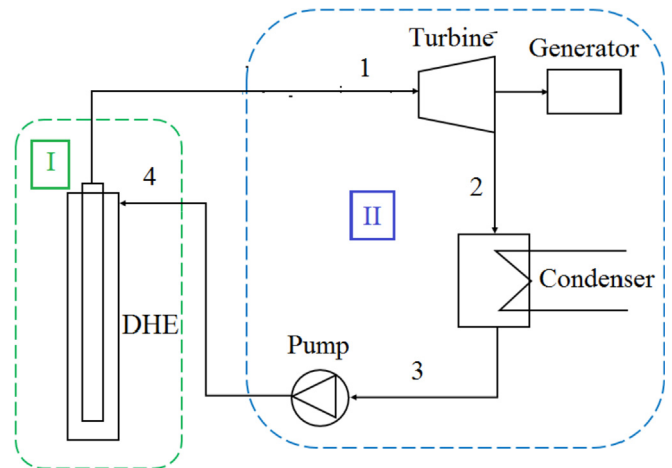

Fig. 5. Temperature profile of the geothermal fluid in the existing well.

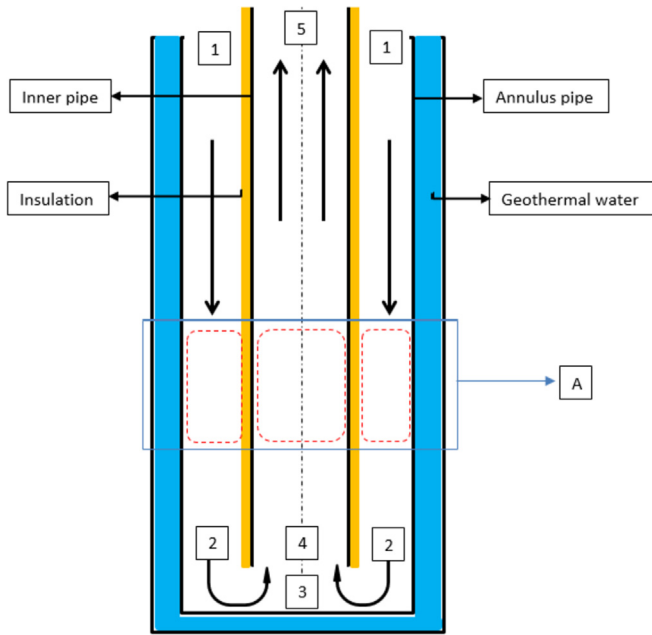**Fig. 6.** Schematic of the GPP-DHE [31].

Fig. 7. Schematic of the DHE [31].

transport property database that is provided for hundreds of substances in a manner that allows it to be used with the equation solving capability.

4.1. Thermodynamic model

Thermodynamic model of the GPP-DHE is based on the ε-NTU method. As it can be seen from Fig. 7, DHE is analyzed according to 5 main sections (1: surface of the annulus pipe, 2: bottom of the annulus pipe, 3: bottom of the DHE, 4: bottom of the inner pipe, 5: surface of the inner pipe) and the relations are derived for these main sections. The DHE is divided into 50 m (dL) sections and output of a section is taken as the input of the next section (Fig. 8). Overall thermal resistance is described into three components: 1) inner pipe-annulus, 2) annulus-geothermal fluid, and 3) geothermal fluid-rock formation. The third resistance is neglected because of steady-state operation assumption and created resistance between geothermal fluid and surrounding rock by casing and cement layer. Cement (0.7–0.9 W/mK) [33] and rock formation (average 2–3 W/mK) [34] have low conductivity similar to Ref. [35]. Energy balance is conducted for cross-section (A) in Figs. 7–8. As can be seen from the Fig. 8, two heat flows exist, one is from

geothermal fluid to the annulus (q_1), the other one is from the inner pipe to the annulus or vice-versa (q_2) (Fig. 8).

The assumptions made for the model construction are;

- Energy balance is under steady-state, steady-flow conditions.
- Fluid is assumed as single phase.
- The geothermal fluid is in liquid phase.
- Thermal process in the geothermal fluid is governed by natural convection process and assumed as pure water.
- Flowrate of the working fluid is constant.
- Temperature profile of the geothermal fluid is assumed as linear by using thermal gradient.
- q_2 is neglected because of the insulation on the inner pipe.

4.1.1. Calculation of convective heat transfer coefficients

Geothermal fluid flows "naturally" in the well as it is driven by buoyancy effect which arises from density differences as consequences of temperature and concentration gradients within the fluid.

The first step of the thermodynamic analysis is to determine the temperature of the geothermal fluid (water), T_w, in the well per section (every 50 m depth) by using temperature gradient value.

After determining the related thermodynamic properties by using water temperature in the well, Nusselt number on a vertical plate can be calculated by Eqs. (1) and (2) [36].

$$Nu = 0.508Ra^{1/4}\left(\frac{Pr}{0.952 + Pr}\right)^{1/4} \text{ if } (Gr < 10^9) \text{ (for laminar flow)}$$

(1)

$$Nu = 0.0295(Ra)^{2/5}\frac{Pr^{1/15}}{(1 + 0.494Pr^{2/3})^{2/5}} \text{ if } (Gr > 10^9) \text{ (for turbulent)}$$

(2)

Ra is the local Rayleigh number which is defined by Eq. (3) [37].

$$Ra = Gr.Pr$$ (3)

where,

$$Gr = \frac{g.\beta.(T_w - T_{ave}).dL^3}{\nu}$$ (4)

T_{ave} is the average temperature of water and working fluid at the same level.

Finally, heat transfer coefficient of the well, h_w, can be calculated by Eq. (5) [37].
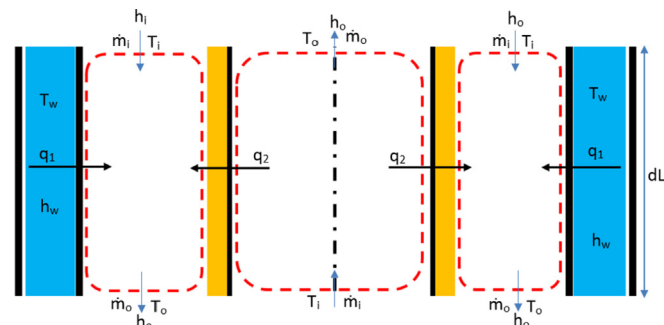
$$h_w = \frac{Nu.k}{dL}$$ (5)

4.1.2. The ε-NTU method for DHE analysis

Working fluid inlet temperature to the DHE is determined by its pressure which is the exit pressure of the circulation pump of the binary cycle.

Working fluid flows in the annulus and inner pipe by forced convection while natural convection exists in the geothermal well. Laminar and turbulent forced convection correlations for single phase fluids represent a significant class of heat transfer solutions for heat exchanger analyses.

After determining required thermodynamic properties of working fluid by using inlet temperature, Nusselt number should

Fig. 8. Heat flow diagram of two control volumes (q_1 and q_2) of the cross section A [31].

be calculated. The Nusselt number for laminar flow, fully developed with a constant surface temperature is 3.66 for $Pr \geq 6$. If $10^4 < Re < 5 \times 10^6$ and $0.5 < Pr < 2000$ while the Nusselt number for turbulent fully developed flow becomes as Eq. (6) [37].

$$Nu = \frac{(f/8).(\text{Re} - 1000).\text{Pr}}{1 + 12.7(f/8)^{1/2}.(\text{Pr}^{2/3} - 1)} \qquad (6)$$

where f is the friction coefficient that can be obtained from the Moody chart that provided by EES software database or by Eq. (7) [37].

$$f = (0.79 \ln \text{Re} - 1.64)^{-2} \qquad (7)$$

h_f which is the convective heat transfer coefficient of working fluid, can be determined using Eq. (8).

$$h_f = \frac{Nu.k}{D_h} \qquad (8)$$

The overall heat transfer coefficient, U, of the annulus and inner pipe are calculated by Eqs. (9) and (10), respectively [37].

$$U_a = \frac{1}{\frac{1}{h_f} + \frac{D_a}{k_a} \ln \frac{D_{a,o}}{D_a} + \frac{D_a}{D_{a,o}.h_w}} \qquad (9)$$

$$U_t = \frac{1}{\frac{1}{h_f} + \frac{D_t}{k_t} \ln \frac{D_{t,o}}{D_t} + \frac{D_t}{k_{ins}} \ln \frac{D_{t,ins}}{D_{t,o}} + \frac{D_t}{D_{t,ins}.h_{f,o}}} \qquad (10)$$

The number of transfer units (NTU) is based on the concept of heat exchanger effectiveness, can be used for DHE analysis and calculated by Eq. (11) [37].

$$NTU = \frac{U.A}{C_{\min}} \qquad (11)$$

where $C_{\min}$ represent minimum heat capacity rate of water and working fluid.

Effectiveness (ε) of DHE for counter and parallel flow can be calculated using NTU method [37].

$$\varepsilon = \frac{1 - \exp[-(1 - C^*)NTU]}{1 - C^* \exp[-(1 - C^*)NTU]} \text{ for counter flow} \qquad (12)$$

$$\varepsilon = \frac{1 - \exp[-(1 + C^*)NTU]}{1 + C^*} \text{ for parallel flow} \qquad (13)$$

where C^* is capacity ratio that is calculated by Eq. (14).

$$C^* = \frac{C_{\min}}{C_{\max}} \qquad (14)$$

$\dot{Q}_{\max}$ is maximum heat transfer rate that can be calculated using Eq. (15).

$$\dot{Q}_{\max} = C_{\min}.(T_w - T_i) \qquad (15)$$

where T_w is water temperature in the well and T_i is inlet temperature of the working fluid.

The actual heat transfer rate is determined by using effectiveness and maximum heat transfer rate [38]:

$$\dot{Q} = \varepsilon.\dot{Q}_{\max} \qquad (16)$$

Consequently, exit temperature of working fluid can be calculated using Eq. (17). This exit temperature is taken as inlet temperature of next section of DHE and the above calculations are repeated for this new inlet temperature.

$$T_o = T_i + \frac{\dot{Q}}{C_{\min}} \qquad (17)$$

4.1.3. Pressure drop calculations

Pressure drop of a vertical cylinder pipe (Fig. 9) can be identified by three components; hydrostatic pressure drop (due to gravity) (Eq. (18)), frictional pressure drop (Eq. (19)) and kinetic pressure drop (Eq. (20)) [39]. Kinetic pressure losses are minimal for most of the applications, therefore can be neglected. In this study, kinetic pressure losses at the inlet and exit of DHE are neglected.

In downward flow, frictional effects exist against the direction of the flow, but effective hydrostatic column helps fluid to overcome such frictional losses. Hydrostatic pressure drop is a function of density of the fluid and frictional pressure drop depends on the fluid properties and flowing conditions within the pipe.

$$\Delta P_{gravity} = \rho.g.dL \qquad (18)$$

$$\Delta P_{friction} = \frac{f.\rho.dL.V^2}{2D_h} \qquad (19)$$

$$\Delta P_{kinetic} = \frac{\rho.(\Delta V)^2}{2} \qquad (20)$$

Pressure drop due to gravity occurs in the open systems, but it will cancel each other when it is a closed system if $\rho_{annulus} = \rho_{inner\ pipe}$. Since, the DHE is being heated by hot geothermal fluid, ρ will change with temperature and pressure increase so that pressure drop due to gravity still exists. At the bottom of the DHE, a kinetic pressure drop occurs due to a change in the flow area. Hence, pressure drop at the bottom of the DHE is caused by kinetic pressure drop.

Pressure output (P_o) along the heat exchanger (L) can be determined with existing pressure drops, represented in Fig. 8, by using Eq. (21).

$$P_o = P_i + \Delta P \qquad (21)$$

4.1.4. Power generation calculations

Once the working fluid leaves the DHE, it is sent to the power plant to generate electricity. The power plant corresponds to Part II in Fig. 6, operates on the Rankine cycle. Main components of power generation system consist of a turbine and generator system, a condenser, and a feed pump.

The actual turbine power generation is calculated by Eq. (22) [40].

$$\dot{W}_t = \dot{m}.(h_1 - h_2).\eta_g \qquad (22)$$

where, $\dot{m}$ is mass flowrate of the fluid, kg/s; h_1 is specific enthalpy of the fluid at turbine inlet, kJ/kg; h_2 is specific enthalpy of the fluid at turbine exit, kJ/kg; η_g is generator efficiency.

The power needed for feed pump to circulate working fluid into the DHE is calculated by Eq. (23) [40].

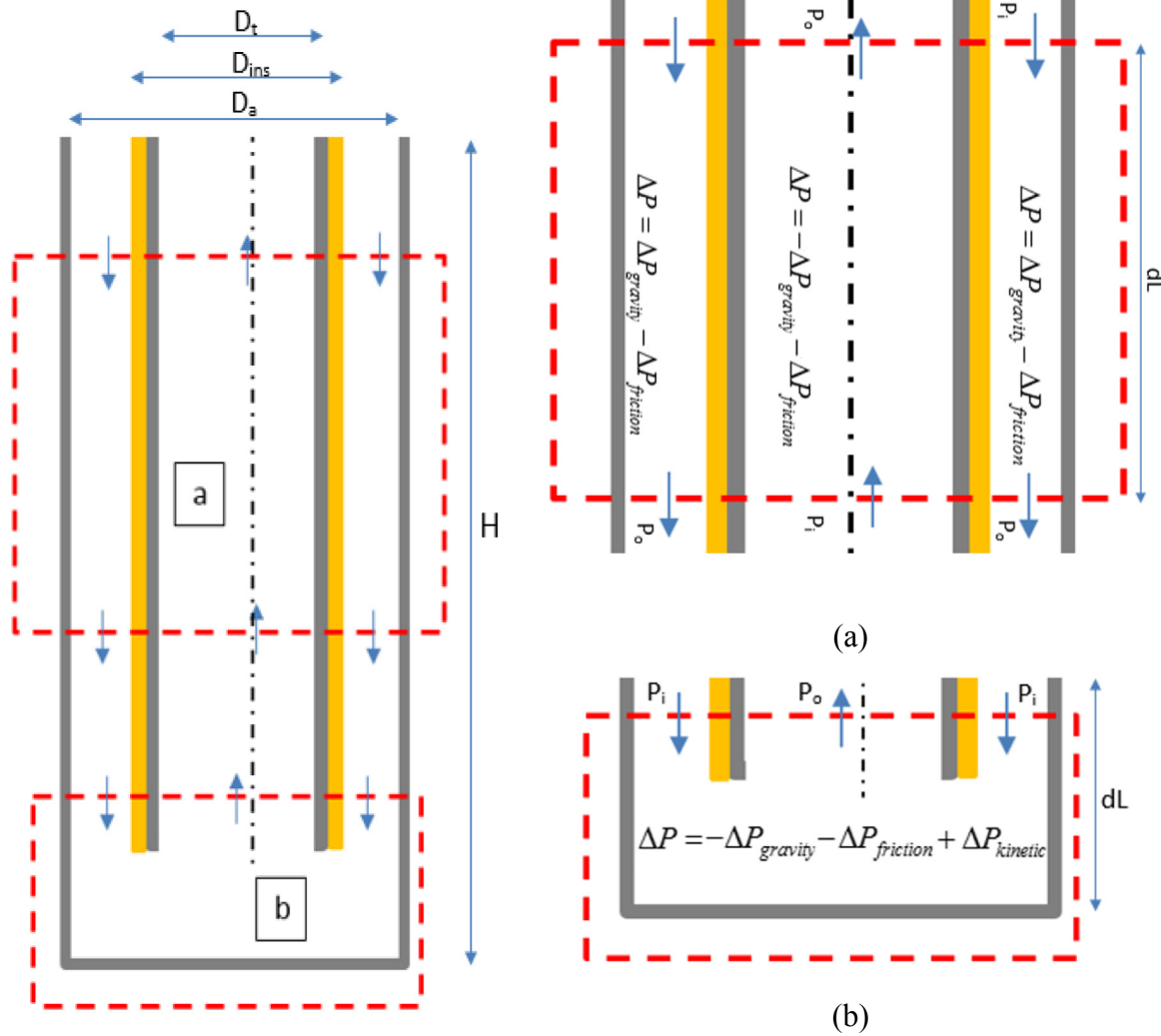$$\dot{W}_p = \dot{m}.(h_4 - h_3)\Big/\eta_p \qquad (23)$$

Fig. 9. Details of pressure drops in the channel of DHE; (a) pressure drop in the main channel (annulus and inner pipe region), (b) pressure drop in the bottom.

Consequently, thermal efficiency of power generation system can be calculated by Eq. (24) [40].

$$\eta_{th} = \frac{\dot{W}_{net}}{\dot{Q}} = \frac{\dot{W}_t - \dot{W}_p}{\dot{Q}} \tag{24}$$

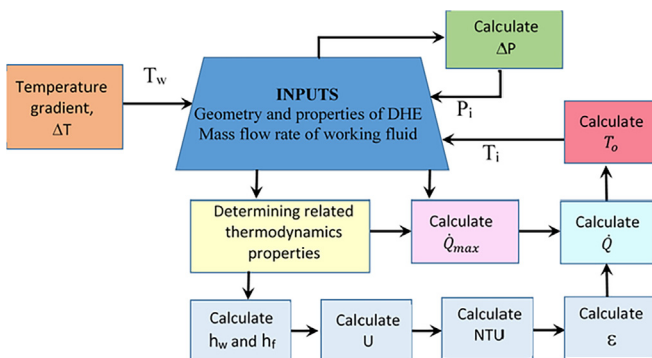The methodology of thermodynamic model of the DHE is summarized in Fig. 10.

Fig. 10. Methodology flow diagram of the thermodynamic model.

4.2. Economic analysis

In this study, net present value (NPV) and simple payback time (SPT) methods are used and electricity generation cost (EPC) is determined to evaluate whether if DHE power generation is competitive or not, comparing with other energy resources.

The NPV is the difference between present value of future cash flows and amount of investment. It is an assessment of expected addition to the investment wealth and used to decide whether an investment is profitable or better than other investments [41]. The NPV is expressed as Eq. (25) [42].

$$NPV = \sum_{n=k+1}^{t} \frac{B_n}{(1+i)^n} - \sum_{n=0}^{k} \frac{C_n}{(1+i)^n} \tag{25}$$

The project is feasible when NPV is positive or greater than zero. Otherwise, the project is unfeasible.

The SPT refers to a period of time required to recover initial investment, or to reach break-even point. The method used to calculate simple economic payback time can be expressed as Eq. (26) [42].

$$SPT = \frac{CIC}{AR - AOMC} \qquad (26)$$

where CIC is capital investment cost, AR is annual revenue and AOMC is annual operation and maintenance cost.

5. Results

5.1. Validation of the model

An EES code was written for thermodynamic model and the model was compared with the literature for validation. Guillaume (2011) installed a coaxial downhole heat exchanger (CDHE) into a geothermal well at 184 m depth. The author monitored the system taking measurements and also modelled the system by COMSOL software. The model was validated by measurements [43]. Since there is no installed system in our study, we compared our EES code with above mentioned study.

The comparison between EES model and Guillaume (2011) which contains measurements and validated COMSOL model, is shown in Fig. 11 and Table 1. It could be easily said that the EES model has lower relative deviations than the COMSOL model, therefore the EES model is accepted as validated.

5.2. Thermodynamic model results

The effects of insulation, temperature gradient and depth of the well, DHE geometry, mass flowrate and type of working fluids on net power generation are investigated by conducting parametric studies with more than 300 simulations. The properties of the system of base case are listed in Table 2.

5.2.1. Effect of insulation thickness

The inner pipe should be insulated to decrease heat loss to the annulus pipe, the inner pipe should be insulated (Fig. 7). Insulation material is chosen as glass wool with a cladding. Thermal conductivity of the insulation is taken as 0.043 W/mK. The insulation is installed at any location where temperature of the annulus pipe is lower than temperature inside the inner pipe. Insulation causes an increase in conduction resistance to heat transfer while decreasing convection resistance of the surface because of the increased outer surface area. The effects of insulation on the temperature distribution along 2500 m deep DHE are examined by taking various insulation thicknesses of the inner pipe and the results are illustrated in Fig. 12. The arrows on the Fig. 12 represents the working

Table 1
Summary of the comparison among measurement, Comsol and EES model.

	T_{in} (°C)	T_{out} (°C)	Relative deviation of temperature distribution (%)	
			Flow down	Flow up
Measurement	4.77	6.35		
COMSOL model	4.77	7.2	1.89	5.56
EES model	4.77	6.48	1.98	1.23

Table 2
Geometrical and thermal properties of base case of the DHE system.

| Parameter	Value
Diameter of the well (m)	0.254
Depth of the DHE (m)	2500
Internal diameter of the annulus pipe (m)	0.2032
Thickness of the annulus pipe (mm)	8.18
Internal diameter of the inner pipe (m)	0.127
Thickness of the inner pipe (mm)	6.55
Temperature gradient of the geothermal fluid (°C/100 m)	6
Thermal conductivity of the insulation (W/mK)	0.043
Thermal conductivity of the annulus and inner pipes (W/mK)	51
Working fluid	R134a
Geothermal fluid temperature at inlet of the DHE (°C)	13.89
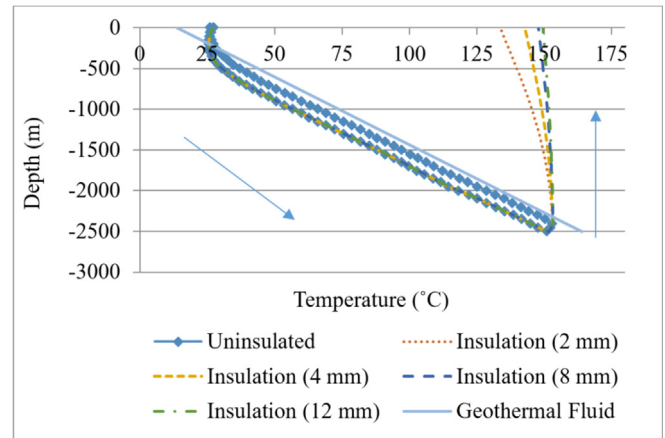
Fig. 12. Effect of insulation on the temperature distribution of the DHE. (Working fluid: R134a, ṁ: 30 kg/s, ΔT: 6 °C/100 m).

fluid flow direction. The results indicate that temperature output of the DHE without insulation is significantly decreased to 26.3 °C at the surface. However, when the DHE is insulated, temperature output can be kept at 133.7 °C for 2 mm insulation thickness and it increases by adding more insulation thickness.

Moreover, the presence of insulation is desirable to maintain pressure output, since density of working fluid is proportional to pressure drop along the channel. Without insulation, pressure drop along inner pipe channel is very high due to increasing density, whereas the density of working fluid is a function of temperature and pressure. Hence, the DHE performance is strongly affected by insulation.

Nonetheless, adding more thickness of insulation on the inner pipe will decrease the volume/area in the annulus region, which mainly affect mass flowrate of working fluid (Fig. 13). Since mass flowrate is a desirable parameter in DHE design, an insulation thickness with relatively minimum heat loss and high flowrate must be selected. The thickness of insulation corresponding to the critical radius of insulation is known as critical insulation thickness.
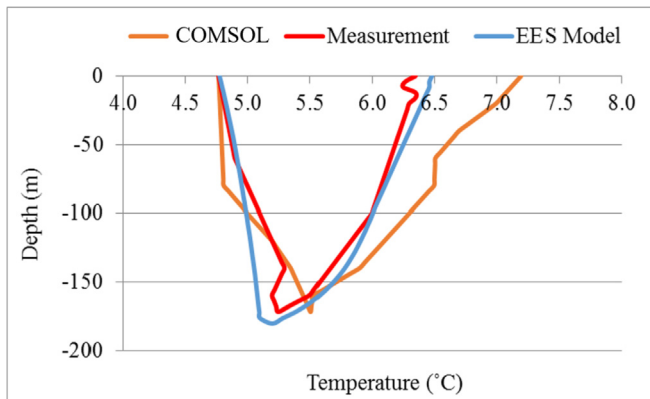
Fig. 11. Temperature distribution between measurement, COMSOL and EES model. (Working fluid: water, flow rate: 2.1 kg/s).
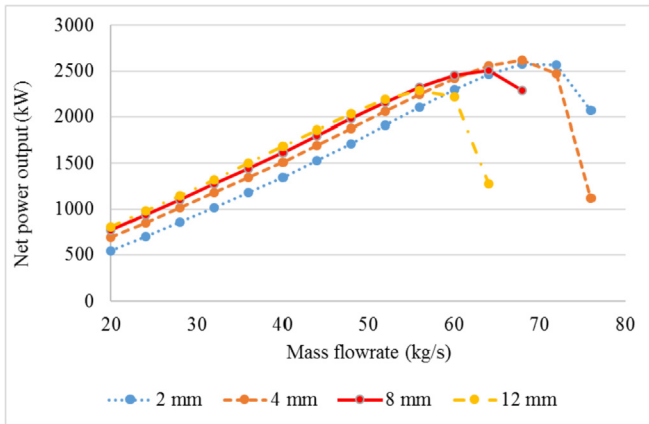
Fig. 13. Effect of insulation thickness to the mass flowrate of working fluids. (Working fluid: R134a, ΔT: 6 °C/100 m).

Fig. 15. Effect of mass flow rate to work output. (Working fluid: R134a, depth: 2500 m, ΔT: 6 °C/100 m).

The critical insulation thickness is determined as approximately 8 mm. Therefore, 8 mm insulation thickness is used for the following analyses.

5.2.2. Effect of temperature gradient

The effect of temperature gradient of geothermal fluid and well depth is analyzed based on net work output of the power plant. As it can be observed from Fig. 14, net work output of GPP-DHE system (30 kg/s of R134a as working fluid) increases with increasing temperature gradient and DHE depth. As an example, at 8 °C/100 m of temperature gradient, net work output of the turbine increases approximately 37% by an increase of 500 m in DHE depth. Since net work outputs are quite low, it is recommended to use either high temperature gradients (≥6 °C/100 m) or high DHE depth (>2000 m).

5.2.3. Effect of mass flowrate of working fluid

Fig. 15 shows the change of net work output with mass flowrate at various pipe diameters. The smaller inner pipe diameter needs a lower flowrate to prevent high pressure drop of the upward stream in the inner pipe region. Which means, mass flowrate is a significant parameter in designing of the system components. Fig. 15 indicates that maximum net work output (2511 kW$_e$) is obtained with 0.127 m diameter pipe at 64 kg/s.

A parametric study is conducted to exhibit the effect of temperature gradient of geothermal fluid and mass flowrate of the working fluid on net power output and results are presented in
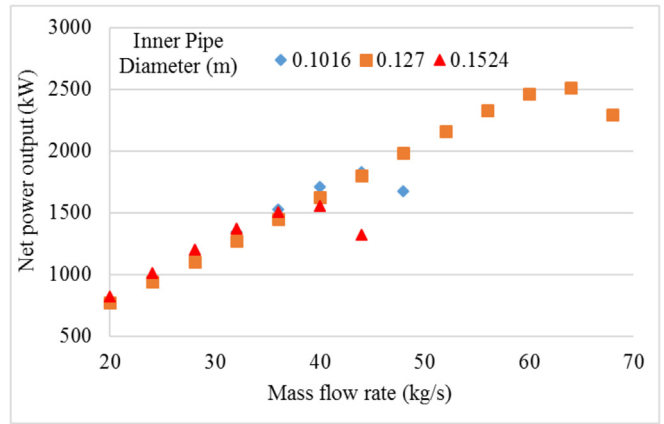

Fig. 14. Effect of temperature gradient of geothermal fluid and depth of DHE to the net work output. (Working fluid: R134a, ṁ: 30 kg/s).

Table 3. The results clearly indicate that increasing temperature gradient and mass flowrate increases turbine work and pump work. But the increase in turbine work is always much greater than pump work. Therefore, net work output always increases. But this is not the case for thermal efficiency. Thermal efficiency increases with temperature gradient. But for the same temperature gradient, increasing flowrate decreases efficiency.

5.2.4. Effect of working fluid type

Effect of working fluid type on system performance is evaluated for six different working fluids such as R134a, R22, R125, R245fa, *n*-Pentane and *n*-Butane. Fig. 16 shows that refrigerants can be operated in higher flowrates than hydrocarbons under given conditions. Therefore, refrigerants deliver higher net work output since work is proportional to mass flowrate. Refrigerant R134a gives the highest net work output (2511 kW$_e$) at optimum mass flowrate of 64 kg/s while other working fluids show lower net work output under the same conditions. On the other hand, Fig. 16 indicates that hydrocarbon working fluids give better performance when the cycle is set at a lower flowrate such as net work output 2060 kW$_e$ can be obtained at 26 kg/s mass flowrate for *n*-Butane.

Thermal efficiency shows performance of a thermodynamic cycle. Fig. 17 illustrates the change of thermal efficiency of considered working fluids with mass flowrate.

Thermal efficiency decreases for all working fluids by increasing mass flowrate. The reduction in flowrate is a result of the improved cycle efficiency with a high resource temperature. There are three working fluids (R134a, R22, and *n*-Butane) that show better performance regarding thermal efficiency (over 19%).

5.3. Economic model results

The DHE power generation system are evaluated based on SPT, EPC and NPV. Changing the geometry of DHE gives different work outputs and costs, which is desirable to understand when a new DHE system is being built.

The CIC of geothermal power plants ranges from 1000 to 4000 $/kW$_e$, depending on the resource characteristics, technology and temperature employed. The CIC components and ranges of GPPs are summarized in Table 4.

Maintenance costs are related to the maintenance of the system components such as pipe networks, turbine, generator, vehicles, buildings and all services. The operation and maintenance cost components and ranges of GPPs are summarized in Table 5.

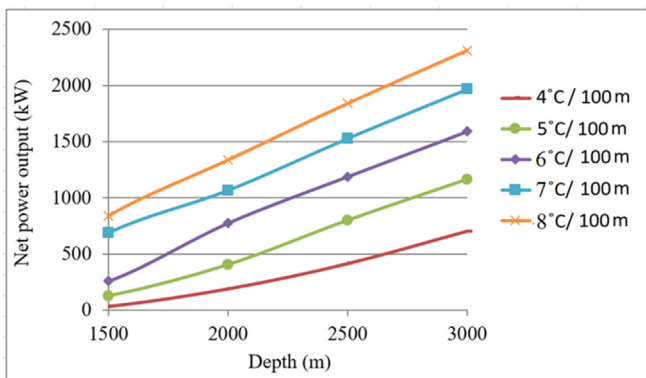For the electricity sales price of 0.105 $/kWh [45], cash flow of

Table 3
Effects of mass flowrate and temperature gradient to net work output.

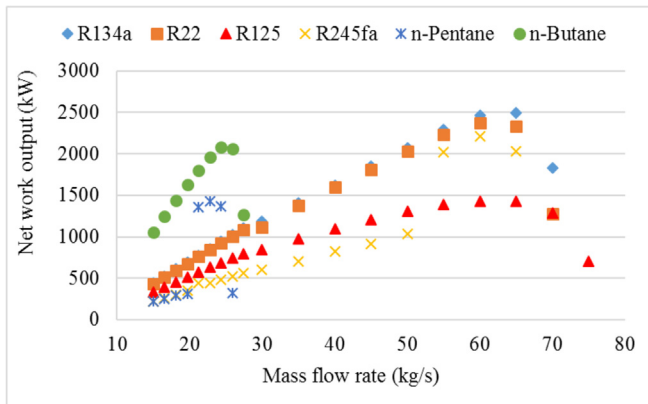| Temperature gradient (°C/100 m)	Mass flowrate (kg/s)	Turbine work (kW$_e$)	Pump work (kW$_e$)	Net work output (kW$_e$)	Thermal Efficiency (%)
5	15	437.5	52.7	384.8	15.54
	30	927.6	105.4	822.2	15.57
	64	2016.0	224.9	1791.1	11.31
6	15	637.1	52.7	584.4	18.65
	30	1329.0	105.4	1223.6	18.68
	64	2735.9	224.9	2511.0	15.39
7	15	823.1	52.7	770.4	20.88
	30	1681.0	105.4	1576	20.69
	64	3297.9	224.9	3073	16.79

Fig. 16. The net work output for various working fluids. (Depth: 2500 m, ΔT: 6 °C/100 m, D$_t$: 0.127 m).
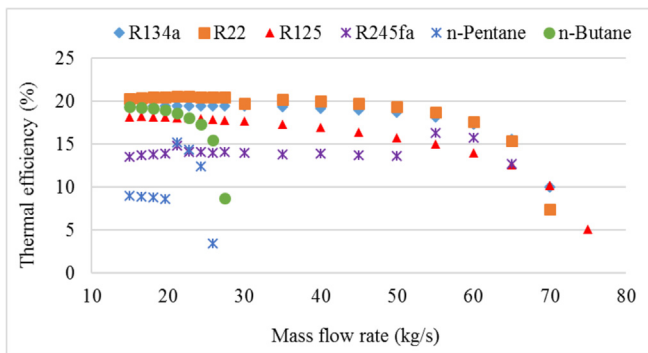

Fig. 17. Thermal efficiency versus mass flowrate. (Depth: 2500 m, ΔT: 6 °C/100 m, D$_t$: 0.127 m).

Table 4
Capital investment cost components and unit cost range [31,44].

Capital Investment Component (CIC)	Cost Range ($/kW$_e$)	Average ($/kW$_e$)	
		Binary	DHE
Exploration	14—263	150	150
Confirmation	150	150	150
Drilling	600—1200	1000	1000
Permitting	565—2030	1000	1000
Design & Construction	1100—2700	1000	1000
Downhole Heat Exchanger	47—70	–	53
Steam Gathering System	30—400	150	50
Transmission		104	104
Total		3554	3507
Sub-Total (if the geothermal well already exists)		1254	1207

Table 5
Operational and maintenance (O&M) cost average value (5% inflation is adjusted) [31,44].

O&M Components	Average Cost (cent$/kWh)
Operating cost	1.1
Power plant maintenance	1.4
Steam field maintenance	1.3
Total	3.8

the plant is calculated for 20 years life span with a stable interest rate at 10% [46]. Optimum design of DHE (2500 m depth with 0.127 m inner pipe diameter) gives the highest net revenue ($1.40 millions) and much faster payback time as 2.25 years for 2511 kW$_e$ net electricity generation and 20.89 GWh annual electricity generation. Total investment and annual O&M costs are determined as $3.14 millions and $0.79 millions, respectively. Electricity generation cost is calculated as 46 $/MWh which is in the range of 43.8—52.1 $/MWh [47].

6. Conclusions

Geothermal power generation requires several wells with geothermal fluid having high temperature and high mass flowrate. Some geothermal wells do not have enough mass flowrate for a feasible power generation even though they have high temperature gradients. These type of wells are generally abandoned although they have potential to generate power by DHEs. DHEs have been used for heating purposes widely but there is no application for electricity generation. Considering the number of wells with abovementioned conditions in the World, there is a potential for electricity generation coupling geothermal power plants with DHEs. Therefore, in this study, thermodynamic and economic models for a geothermal power plant with a coaxial type DHE system has been developed by EES software to examine the possibility of electricity generation from the wells having insufficient mass flowrate and high temperature geothermal fluid. The steady-state models are simulated based on depth and temperature gradient of geothermal heat source, diameter of inner pipe, mass flowrate and type of working fluids. The analyses indicate that characteristics of geothermal heat source, geometry of DHE, optimum mass flowrate and type of working fluids are most influencing parameters on power generation by DHEs. Based on maximum obtainable net work output that can be produced by GPP with DHE, using refrigerant R134a is highly recommended with a net work output of 2511 kW$_e$ for a single well (a depth of 2500 m, a temperature gradient of 6 °C/100 m, an inner pipe diameter of 0.127 m). Optimum mass flowrate of R134a is determined as 64 kg/s. Annual electricity generation is calculated as 20.89 GWh. Since existing thermodynamic model was developed for steady-state operation, geothermal fluid temperature drop with time caused by heat loss to the rock formation is neglected. Another reason for that is the DHE

is installed into a well with casing and cement layer which create a resistance to heat transfer from geothermal fluid to surrounding rocks. Since temperature drop of geothermal fluid directly affects the power generation, it is important to show whether if heat transfer between geothermal fluid and rock formation can be neglected or not. To examine the sustainability of the geothermal heat source, cycle performance along the lifetime of the system, and find out the amount of heat loss to the surrounding rock formation and temperature drop of geothermal fluid with time, a further study is planned to improve the existing model by transient analysis.

Simple payback time and electricity generation cost are computed as 2.25 years and 0.46 $/MWh, respectively. Finally, according to the obtained results of thermodynamic analyses, it can be concluded that DHE system could be a feasible alternative for power generation using abandoned wells.

Acknowledgements

NOMENCLATURE

A	Total heat transfer area (m^2)
AOMC	Annual operation and maintenance cost ($)
AR	Annual revenue ($)
B	Benefit ($)
C	Heat capacity rate (kW/K), cost ($)
CIC	Capital investment cost ($)
D	Diameter (m)
dL	Length (m)
f	Friction factor ($-$)
g	Gravitational acceleration (m/s^2)
Gr	Grashof number ($-$)
h	Heat transfer coefficient ($W/m^2.K$), enthalpy (kJ/kg)
i	Annual interest rate or discount rate ($-$)
k	Thermal conductivity (W/mK)
$\dot{m}$	Mass flow rate (kg/s)
NPV	Net Present Value ($)
NTU	Number of heat transfer unit based on C_{min}, UA/C_{min}
Nu	Nusselt number ($-$)
P	Pressure (kPa)
Pr	Prandtl number($-$)
$\dot{Q}$	Heat flow rate (kW)
Ra	Rayleigh Number ($-$)
Re	Reynolds number($-$)
SPT	Simple payback time (year)
t	The number of the periods for the project exploitation
T	Temperature (^oC, K)
U	Overall heat transfer coefficient ($W/m^2.K$)
V	Velocity (m/s)
$\dot{W}$	Work (kW)

Greek letters

β	Coefficient of thermal expansion
Δ	Gradient, difference
ε	Heat exchanger effectiveness ($-$)
η	Efficiency ($-$)
ν	Kinematic viscosity (Pa.s)
ρ	Density (kg/m^3)

Subscripts

a	annulus pipe
a,o	annulus pipe outer
ave	average
f	working fluid
friction	friction
f,o	working fluid outlet
g	generator
gravity	gravity
h	hydraulic
i	inlet
ins	insulation
kinetic	kinetic
max	maximum
min	minimum
n	number of the years
net	net
o	outlet
p	pump
t	inner pipe, turbine
th	thermal
t,ins	inner pipe insulation
t,o	inner pipe outer
w	water

References

[1] Dave Duchane, Don Brown, Hot Dry Rock (HDR) Geothermal Energy Research and Development at Fenton Hill, New Mexico, vol. 23, Geo-Heat Centre Quarterly Bulletin, 2002.

[2] Gaosheng Wei, et al., Performance analysis on a hot dry rock geothermal resource power generation system based on Kalina cycle, Energy Proc. 75 (2015) 937−945.

[3] John W. Lund, Tonya L. Boyd, Direct utilization of geothermal energy 2015 worldwide review, Geothermics 60 (2016) 66−93.

[4] C. Alimonti, et al., The wellbore heat exchangers: a technical review, Renew. Energy 123 (2018) 353−381.

[5] Haiyan Lei, Xuezhang Liu, Chuanshan Dai, Experiment of heat transfer in downhole heat exchangers with a promoter pipe, GRC Transact. 36 (2012).

[6] John W. Lund, Large Downhole Heat Exchanger in Turkey and Oregon, vol. 20.3, Geo-Heat Center Quarterly Bulletin, 1999.

[7] Jeffrey D. Spitler, Saqib Javed, Randi Kalskin Ramstad, Natural convection in groundwater-filled boreholes used as ground heat exchangers, Appl. Energy 164 (2016) 352−365.

[8] Shabnam Gharibi, et al., Feasibility study of geothermal heat extraction from abandoned oil wells using a U-tube heat exchanger, Energy 153 (2018) 554−567.

[9] David Gordon, et al., Experimental and analytical investigation on pipe sizes for a coaxial borehole heat exchanger, Renew. Energy 115 (2018) 946−953.

[10] Tomasz Sliwa, Marc Rosen, Natural and artificial methods for regeneration of heat resources for borehole heat exchangers to enhance the sustainability of underground thermal storages: a review, Sustainability 7 (10) (2015) 13104−13125.

[11] José Acuña, Improvements of U-Pipe Borehole Heat Exchangers, Diss, KTH, 2010.

[12] E. Zanchini, S. Lazzari, A. Priarone, Improving the thermal performance of coaxial borehole heat exchangers, Energy 35 (2) (2010) 657−666.

[13] Xianzhi Song, et al., Numerical analysis of the heat production performance of a closed loop geothermal system, Renew. Energy 120 (2018) 365−378.

[14] Peixue Jiang, et al., Heat extraction of novel underground well pattern systems for geothermal energy exploitation, Renew. Energy 90 (2016) 83−94.

[15] Gioia Falcone, et al., Assessment of deep geothermal energy exploitation methods: the need for novel single-well solutions, Energy 160 (2018) 54−63.

[16] A.B. Alkhasov, et al., Prospects for use in exhausted petroleum fields of borehole heat exchangers and artesian water-bearing horizons for supplying heat and hot water, Therm. Eng. 55.12 (2008) 1009−1016.

[17] Gopi Nalla, et al., Parametric sensitivity study of operating and design variables in wellbore heat exchangers, Geothermics 34.3 (2005) 330−346.

[18] Yin Feng, Numerical Study of Downhole Heat Exchanger Concept in Geothermal Energy Extraction from Saturated and Fractured Reservoirs, Ph.D Thesis, University of Louisiana, Lafayette, USA, 2012.

[19] Yin Feng, Mayank Tyagi, Christopher D. White, A downhole heat exchanger for horizontal wells in low-enthalpy geopressured geothermal brine reservoirs, Geothermics 53 (2015) 368−378.

[20] Ildar Akhmadullin, Tyagi Mayank, Design and analysis of electric power production unit for low enthalpy geothermal reservoir applications." World

Academy of Science, Engineering and Technology, Int. J. Environ. Chem. Ecol. Geol. Geophys. Eng. 8 (6) (2014) 443—449.

[21] Koji Morita, Makoto Tago, Sachio Ehara, Case studies on small-scale power generation with the downhole coaxial heat exchanger, in: Proc. World Geothermal Congress, Antalya, Turkey, 2005.

[22] Ali Kilicarslan, Norbert Müller, A comparative study of water as a refrigerant with some current refrigerants, Int. J. Energy Res. 29.11 (2005) 947—959.

[23] Anh, Ngoc Lai, Thermodynamic Data of Working Fluids for Energy Engineering, Diss. Ph. D Thesis, University of Natural Resources, Vienna, Austria, 2009.

[24] Salah Masheiti, Brian Agnew, Sara Walker, An evaluation of R134a and R245fa as the working fluid in an Organic Rankine Cycle energized from a low temperature geothermal energy source, J. Energy Power Eng. 5 (2011) 5.

[25] Chiranjeev Kalra, et al., High-potential working fluids and cycle concepts for next-generation binary organic Rankine cycle for enhanced geothermal systems, in: 37th Workshop on Geothermal Reservoir Engineering, Stanford, CA, Jan. 2012.

[26] Andriy Redko, et al., Efficiency of geothermal power plant cycles with different heat-carriers, in: Proceedings 41st Workshop on Geothermal Reservoir Engineering, Stanford University, Stanford, California, 2016.

[27] Tuğbanur Özen, Bülbül Ali, Gültekin Tarcan, Reservoir and hydrogeochemical characterizations of geothermal fields in Salihli, Turkey, J. Asian Earth Sci. 60 (2012) 1—17.

[28] Rabia Gören, Alaşehir ve çevresinde Gediz grabeni güney kenar faylarının holosen aktivitesi. MS thesis, ESOGÜ, Fen Bilimleri Enstitüsü, 2016.

[29] Hakan Aydın, Serhat Akın, Alaşehir Jeotermal Sahasinin Ayrik Çatlak Ağ modellemesi", in: Proceedings GT 2019 3rd Geothermal Turkey Congress, Ankara, Turkey, 2019 (in Turkish).

[30] Hakki AYDIN, Serhat AKIN, T.E.Z.E.L. Seray, Practical experiences about reservoir monitoring in Alaşehir geothermal field, in: Proceedings of 43rd Workshop on Geothermal Reservoir Engineering, Stanford University, Stanford, California, 2019.

[31] Slamet Parmanto, Thermodynamic Optimization of Downhole Heat Exchangers for Geothermal Power Generation, MS thesis, Izmir Institute of Technology, 2016.

[32] S.A. Klein, F.L. Alvarado, EES-engineering Equation Solver, F-chart software, 2002.

[33] Fuzong Zhou, Research on Heat Transfer in Geothermal Wellbore and Surroundings, Ph. D. Thesis, Faculty of Planning Building Environment, Technical University of Berlin, 2013.

[34] Elif Balkan, Kamil Erkan, Müjgan Şalk, Thermal conductivity of major rock types in western and central Anatolia regions, Turkey, J. Geophys. Eng. 14 (4) (2017) 909—919.

[35] Aleks D. Atrens, Hal Gurgenci, Victor Rudolph, Electricity generation using a carbon-dioxide thermosiphon, Geothermics 39.2 (2010) 161—169.

[36] Sadık Kakaç, Ramesh K. Shah, Win Aung, Handbook of Single-phase Convective Heat Transfer, Wiley New York et al, 1987.

[37] F.P. Incropera, D.P. DeWitt, Introduction to Heat Transfer, fourth ed., Wiley, New York, 2002.

[38] Sadik Kakaç, Hongtan Liu, Anchasa Pramuanjaroenkij, Heat Exchangers: Selection, Rating, and Thermal Design, CRC press, 2002.

[39] Mahmoud Massoud, Engineering Thermofluids, vol. 2005, Springer-Verlag Berlin Heidelberg, 2005.

[40] Yunus A. Cengel, Introduction to Thermodynamics and Heat Transfer, McGraw-Hill, New York, 2008.

[41] Ayşe Konyalı, Financial Evaluation of Kızıldere Geothermal Power Plant, MS thesis, Izmir Institute of Technology, 2010.

[42] Yıldırım Özcan, Nurdan, Modeling, Simulation and Optimization of Flashed-Steam Geothermal Power Plants from the Point of View of Noncondensable Gas Removal Systems, 2010.

[43] F. Guillaume, Analysis of a Novel Pipe in Pipe Coaxial Borehole Heat Exchanger, KTH School of Industrial Engineering and Management. Sztokholm (Szwecja), 2011.

[44] Hance, Cédric Nathanaël, Factors Affecting Costs of Geothermal Power Development, Geothermal Energy Association, 2005.

[45] Law on Amendments on the Law on Utilization of Renewable Energy Resources for the Purpose of Generating Electrical Energy, Law no: 6094, Official gazette, Date Ratified: 29/12/2010, http://www.resmigazete.gov.tr/eskiler/2011/01/20110108-3.htm.

[46] Turkey: Development of Short-Term Annual Interest Rate from 2009 to 2018, https://www.statista.com/statistics/418828/annual-short-term-interest-rate-in-turkey/(access in 2018).

[47] E.I.A. Levelized, Avoided Cost of New Generation Resources in the Annual Energy Outlook, 2015 (Retrieved from USA).